Adsorption (2015) 21:467–478
DOI 10.1007/s10450-015-9687-3

Ideal cascade theory applied to carbon monoxide isotope separation by pressure swing adsorption

Shubhra J. Bhadra[1] · Armin D. Ebner[1] · Vincent van Brunt[1] · James A. Ritter[1]

Received: 2 July 2015 / Accepted: 6 July 2015 / Published online: 10 July 2015

Abstract A three-step design methodology was developed for applying ideal cascade theory to separate a dilute binary gas mixture by pressure swing adsorption (PSA). This methodology was tested via simulation and applied to the enrichment of ^{14}CO from 1 to 20 ppm in a mixture of its own isotopes. It was assumed that the presence and slight enrichment of ^{13}CO did not affect the performance of ^{14}CO throughout the cascade. An 8 stage cascade was analyzed, with 3 stages in the stripping section, 5 stages in the enriching section and the feed fed to stage 4. Each stage consisted of a 3-bed 3-step PSA process of varying size, all utilizing feed pressurization/feed, heavy reflux and countercurrent depressurization steps of equal duration, and the same total cycle time. The performance in terms of overall ^{14}CO recovery from an ideal cascade of PSA units was compared to that from a single PSA unit operating with the same overall ^{14}CO enrichment and same overall throughput as the cascade. The results showed that the cascade of PSA units compared to the single PSA unit exhibited increasingly higher overall recoveries as the overall enrichment decreased; the performance of both systems became identical at an overall enrichment of about 18; and at overall enrichments higher than 18 the single PSA unit exhibited only slightly higher overall recoveries than the cascade of PSA units. The better performing separation process in either case always required more power to operate. In general, this analysis showed how to design an ideal cascade of PSA units for binary isotope separation and that a cascade of PSA units may be more advantageous than a single PSA unit, depending on the desired performance and as long as the capital and operating costs are acceptable.

Keywords PSA · Cascade theory · Isotope separation · Pressure swing adsorption

Notation

D_i	Depletion of species of interest at stage i
E_i	Enrichment of species of interest at stage i
F	Primary feed flow of the PSA cascade
F_i	Feed flow to stage i
HP_i	Heavy product flow at stage i
I	Stage i
L_i	Tail flow in the depleted stream at stage i or loss of species of interest at stage i
LP_i	Light product flow at stage i
M	Total number of stages in stripping section
N	Total number of stages in enriching section
N	Total number of moles exiting the bed during the CnD step
n_i	Total number of moles exiting the bed during the CnD step at stage i
N_T	Total number of stages in the cascade
P	Head or enriched product flow from the PSA cascade
P_i	Head or enriched product flow from stage i
P_{i-1}	Head or enriched product flow from stage $i - 1$
R_i	Recovery of species of interest at stage i
R_R	Heavy product reflux ratio
$R_{R,i}$	Heavy product reflux ratio at stage i
t_{step}	Duration of production step
v	Volume of each PSA bed
v_i	Volume of PSA bed at stage i
V_i	Head flow in the enriched stream at stage i

✉ James A. Ritter
ritter@cec.sc.edu

[1] Department of Chemical Engineering, University of South Carolina, Columbia, SC 29208, USA

W	Tail or lean product flow from PSA cascade
W_i	Tail or lean product flow from stage i
W_{i+1}	Tail or lean product flow from stage $i + 1$
x_i	Depleted stream composition of strongly adsorbed species at stage i
x_{i+1}	Depleted stream composition of strongly adsorbed species at stage $i + 1$
x_{i+2}	Depleted stream composition of strongly adsorbed species at stage $i + 2$
X_i	Molar ratio of strongly adsorbed species of depleted stream at stage i
x_w	Depleted product composition of strongly adsorbed species
y_i	Enriched stream composition of strongly adsorbed species at stage i
y_{i-1}	Enriched stream composition of strongly adsorbed species at stage $i - 1$
y_{i-2}	Enriched stream composition of strongly adsorbed species at stage $i - 2$
Y_i	Molar ratio of strongly adsorbed species of enriched stream at stage i
y_P or y_p	Enriched product composition of strongly adsorbed species
z_i	Feed composition of strongly adsorbed species at stage i
z_{i+1}	Feed composition of strongly adsorbed species at stage $i + 1$
z_{i-1}	Feed composition of strongly adsorbed species at stage $i - 1$
Z_i	Molar ratio of strongly adsorbed species of feed stream at stage i
z_F or z_f	Primary feed composition of strongly adsorbed species

Greek letters

ρ_b	Bulk density of the bed
α_i	Separation factor of stage i
β	Head or tail separation factor
$\beta_{1,i}$	Head separation factor
$\beta_{2,i}$	Tail separation factor
θ	Constant stage throughput ($\theta_i = \theta =$ constant)
θ_i	Stage throughput
$\theta_{overall}$	Overall throughput (cascade or single PSA unit)
ψ	Total number of moles exiting the bed during the CnD step per volume of bed

1 Introduction

Many of the world's 443 nuclear reactors, with a rated capacity of approximately 365 GW of electricity, use graphite as a moderator, reflector, and/or fuel matrix. About 250,000,000 kg of spent graphite exists and is contaminated with around 1 ppm of the long half-life radio-nuclide, ^{14}C. Because the spent graphite contains ^{14}C, it is considered as a high-level radioactive waste (Fachinger et al. 2008). To safely and rationally dispose of it in a cost-effective manner, technology is needed to reduce the volume of the ^{14}C radioactivity.

Among the different technologies being proposed for volume reduction, gasification of the graphite to CO or CO_2, with subsequent separation of the carbon isotopes, is being viewed as one of the more promising methods (Mason and Bradbury 2002). The off gas from graphite gasification would contain all the isotopes of carbon, i.e., ^{12}C, ^{13}C and ^{14}C, as CO or CO_2. Hence, an isotope separation technique is needed that would selectively concentrate ^{14}C from ^{12}C and ^{13}C.

Gaseous isotope separation techniques include the use of centrifugal, (Cohen and Kaplan 1942; O'Farrell 1981; Whitley 1984; Kholpanov et al. 1997) diffusional, (Pratt 1967; Lonsdale 1982; Applegate 1984; Geankoplis 2003) gas chromatography, (Cheh 1994) gas adsorption, (Keshaviah 1972; Patrick et al. 1972; Hill and Grzetic 1983; Izumi et al. 2005; Bhadra and Ebner 2013) distillation, (Benedict et al. 1981; McInteer 1978; Chang et al. 1994) and electrolysis and laser devices (Robieux and Auclair 1965; Letokhov 1970; Ambartsumian et al. 1974). Among these various isotope separation techniques, only the centrifugal and diffusional methods have been commercialized and mostly for medical applications. In addition to these, gas adsorption techniques have been used for isotope separation by the US government in defense applications (Horen and Lee 1991; Ortman et al. 1989; Shanahan et al. 1999). For the particular case of carbon isotope separation, pressure swing adsorption (PSA) has recently been shown to be a viable option for the concentration of ^{14}C in pure CO streams (Izumi et al. 2005; Bhadra and Ebner 2013).

The design of a separation process using the principle of a cascade is an attractive concept for separating isotopes that naturally have a separation factor very close to unity (Benedict et al. 1981). Theoretically, a cascade is usually analyzed based on the principle of an ideal stage. A classical analysis of such a design is presented by Cohen (1951) based on the principle of an ideal cascade.

Conceptually, the ideal cascade approach minimizes both the inter-stage flow and cost for a specific application. The analysis provides not only the number of stages or the size and number of beds but also the inter-stage flows and compositions required for a particular separation. The ideal cascade theory by Cohen (1951) has been successfully applied to uranium isotope separation by the gaseous diffusion method (Pratt 1967), tungsten isotope separation by the centrifugal gas technique (Kholpanov et al. 1997) and hydrogen isotope separation by gas adsorption (Hill and Grzetic 1983).

Surprisingly, the use of classical ideal cascade theory applied to the design of an isotope separation process based on PSA is lacking. Therefore, the primary objective of this study is to provide a three-step methodology for designing an ideal cascade of PSA units via simulation. In particular, the methodology for ideal cascade applied to an assumed binary gas mixture of isotopes is utilized for the concentration and removal of ^{14}CO from an isotopic mixture of all three carbon isotopes using a known PSA cycle that has been previously utilized for this separation (Bhadra and Ebner 2013). In such an approach it is assumed that the presence and slight enrichment of ^{13}CO does not alter the performance of ^{14}CO throughout the cascade, thereby making binary cascade theory applicable to this system of isotopes. As a secondary objective, it is shown how to carry out a comparative (but not exhaustive) performance evaluation study to identify whether an ideal cascade of PSA units shows any advantages over a single PSA unit for a difficult isotope separation, when both processes are designed to provide the same performance.

2 Ideal cascade and design strategies for PSA applications

2.1 Cascade fundamentals

A cascade in a PSA process is comprised of a series of different sized, multi-bed PSA units, with each one individually constituting a single stage. Depending on the stage configuration, the cascade may be oriented in a squared-off or tapered fashion. In the former case, the capacity of all stages remains the same, while for the later the capacity of each stage decreases as the enriched or depleted end is approached. An ideal cascade is nothing but an idealized version of a tapered plant designed to gather various insights into the system as well as to minimize the separation cost. The theory behind the ideal cascade was developed by Cohen (1951); its salient features are reiterated here for the sake of completeness.

A comprehensive feature of the ideal cascade design for a binary gas mixture is presented in the schematic shown in Fig. 1, where a series of interconnected stages are arranged to form an ideal cascade. The cascade receives a primary feed stream F that contains a species of interest with concentration z_F, and produces a head stream P enriched in the species of interest with concentration y_P, and a tail stream W depleted in the species of interest with concentration x_W. Each rectangular box in the figure corresponds to a stage representing a multi-bed PSA unit. It is assumed here that these PSA units only vary in volume from stage to stage; they all operate using the same cycle time, cycle schedule and number of beds. The feed (F_i), head (P_i) and

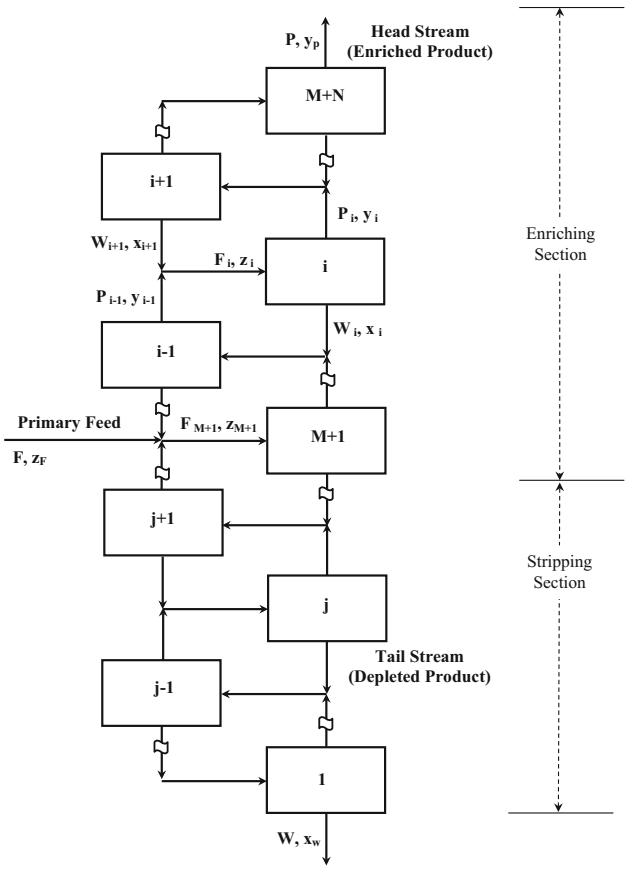

Fig. 1 Schematic representation of an ideal cascade consisting of $M + N$ stages: in distillation a series of interconnected plates or stages constitutes a cascade, whereas in PSA a series of different sized, multi-bed PSA units constitutes a cascade, with each PSA unit being a stage

tail streams (W_i) for stage i are represented by the horizontal, upward and downward arrows, respectively. The concentrations for the species of interest for these streams are defined as z_i, y_i and x_i. The sections above and below the primary feed (F) location are called the enriching and stripping sections, each consisting of N and M PSA units, respectively. Except for the stage receiving the primary feed, the feed F_i is the sum of tail and head streams emanating from one stage above and one stage below, i.e., $F_i = W_{i+1} + P_{i-1}$. At the stage receiving the primary feed, which is stage i, $i = M + 1$ and $F_i = F + W_{i+1} + P_{i-1}$.

Two important features define an ideal cascade (Cohen 1951). The first feature is called the *no mixing criterion*, where it is assumed that the head and tail streams from stages $i - 1$ and $i + 1$, respectively forming a feed stream to stage i, have the same composition, i.e., $z_i = y_{i-1} = x_{i+1}$. The implication of this criterion is that the total interstage flows as well as the total cascade volume are all minimized in such an ideal cascade. The second feature is the assumption of constant separation factor α_i on each stage. This stage separation factor is defined as

$$\alpha_i = \frac{Y_i}{X_i} \tag{1}$$

where $X_i = x_i/(1 - x_i)$ and $Y_i = y_i/(1 - y_i)$ are the molar ratios of tail and head streams of stage i, respectively. A very similar term used in cascade design is the head ($\beta_{1,i}$) and tail ($\beta_{2,i}$) separation factors, which are defined as

$$\beta_{1,i} = \frac{Y_i}{Z_i} \tag{2}$$

$$\beta_{2,i} = \frac{Z_i}{X_i} \tag{3}$$

where $Z_i = z_i/(1 - z_i)$ is the molar ratio in the feed stream of stage i. A pictorial view of these separation factors is presented in Fig. 2. The fundamental definitions of all the separation factors as well as the *no mixing criterion* lead to the relation $\beta_{1,i} = \beta_{2,i} = \beta = \alpha_i^{0.5}$ where β is either the head or tail separation factor. Consequently, the separation factor β remains the same for each stage. It is shown later that β is nothing but the enrichment per stage (i.e., per PSA unit) when the feed concentration of the species of interest is very small.

2.2 PSA unit

As stated earlier, each rectangular box shown in Fig. 1 represents a stage, i.e., a PSA unit of any convenient design, with each one utilizing the same cycle time, cycle schedule and number of beds, while varying in volume. In particular, it is assumed that each one consists of the 3-bed

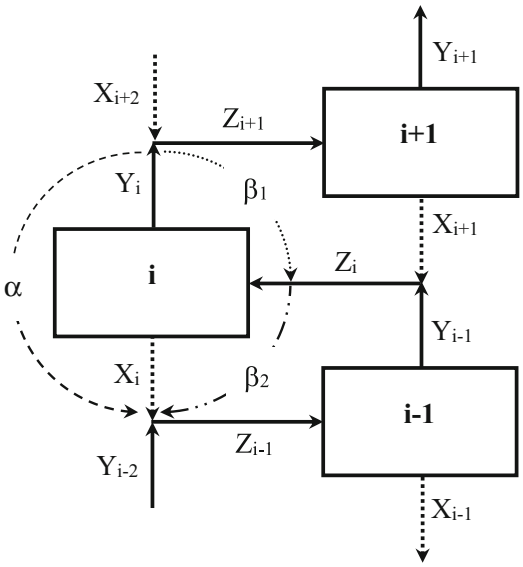

Fig. 2 Schematic representation of different separation factors used in the analysis of an ideal cascade. All the stream compositions entering and leaving stage i, i + 1 and i − 1 are represented in terms of molar ratios

3-step PSA unit studied elsewhere (Bhadra and Ebner 2013) and depicted in Fig. 3. The cycle step sequence for this PSA process consists of a feed pressurization/feed (FP/F) step, a heavy reflux (HR) step and a countercurrent depressurization (CnD) step. Each cycle step has the same duration t_{step}.

During the FP/F step, a bed is initially pressurized from a low pressure to a high pressure by introduction of the feed mixture while maintaining the other end of the bed closed. Upon reaching the upper pressure, the closed end of the bed is opened and the FP/F step continues by allowing the gas to pass through the bed at the high pressure. During the entire step the more strongly adsorbed component is collected in the bed while a stream enriched with the more weakly adsorbed component is recovered as the light product.

During the HR step, the feed end of a bed is fed at the same high pressure of the FP/F step using a fraction of the gas stream produced during the CnD step that is enriched with the more strongly adsorbed component. The fraction fed is defined by the reflux ratio (R_R). The effluent from this HR step is recycled back to the feed. The purpose of this step is to increase further the loading of the more strongly adsorbed component in the bed by flushing the more weakly adsorbed component further up the bed. This, in turn, increases the enrichment of the more strongly adsorbed component during the CnD step.

During the CnD step, the bed is depressurized from the high pressure to the low pressure countercurrently through the feed end with the other end of the bed closed. A fraction of the effluent stream from this step is recovered as the enriched product, while the remaining portion is used as reflux in the HR step. The purpose of this step is to regenerate the bed by removing the more strongly adsorbed component countercurrently.

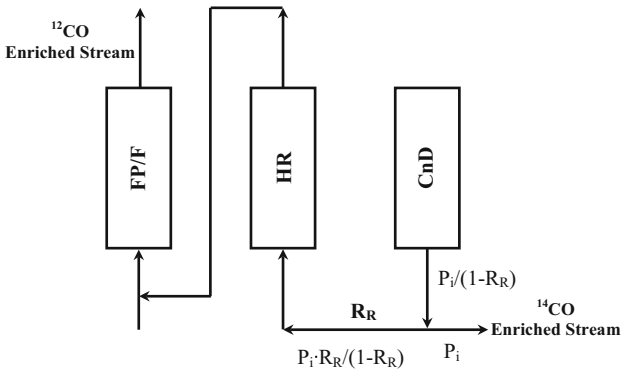

Fig. 3 Schematic of the 3-bed 3-step PSA process (Bhadra and Ebner 2013) developed for ^{14}CO separation from ^{12}CO and ^{13}CO that is used in each stage of the ideal cascade and in the single PSA unit. FP/F: feed pressurization/feed step, HR: heavy reflux step, CnD: countercurrent depressurization step, and R_R: reflux ratio

2.3 Design strategy

In this section, a design methodology is formulated for merging binary ideal cascade theory with PSA principles for dilute systems. To facilitate the formulation, the key features of the design are divided into three steps. Step I involves establishing the number of stages, stage separation factor and overall performance variables required for the separation of a particular binary mixture into two product streams. This is carried out by either defining or determining these variables with the aid of the following relationships (Cohen 1951):

$$M = \frac{\ln \frac{z_f(1-x_w)}{(1-z_f)x_w}}{\ln \beta} - 1 \tag{4}$$

$$N = \frac{\ln \frac{y_p(1-z_f)}{(1-y_p)z_f}}{\ln \beta} \tag{5}$$

The sum $M + N = N_T$ provides the total number of stages (i.e., PSA units) in the cascade. Equations 4 and 5 contain six unknown parameters, namely x_w, z_f, y_p, β, M and N. Clearly, choosing or fixing any four of them resolves the other two by solution of the two equations. In general, because M and N can only be integers, they are selected as part of the four fixed parameters. For example, if the total number of stages in the enriching and stripping sections as well as the primary feed and enriched product compositions are specified, then Eqs. 4 and 5 can be solved for the depleted product composition x_w and head (or tail) separation factor β. The specification of some stream compositions can be done either directly or indirectly by specifying the overall recovery of a species of interest. Finally, the overall and component material balances over the entire cascade provide sufficient information for determining the enriched (P) and depleted (W) product flows and compositions once the primary feed flow rate (F) is specified.

Step II involves determining the inter-stage flows, the inter-stage compositions of the more strongly adsorbed component, and the stage recoveries and enrichments of the species of interest. The internal material balances between any two stages and around one end of the cascade in either the enriching or stripping section, together with the fundamental definition of the separation factor and the *no mixing criterion*, provide a sufficient number of equations for calculating the inter-stage flows and inter-stage compositions. For the enriching section, these equations are given by (Cohen 1951)

$$W_i = \frac{P}{\beta - 1}\left[y_p\left(1 - \frac{1}{\beta^{N-i+1}}\right) + (1 - y_p)\beta\left(\beta^{N-i+1} - 1\right)\right] \tag{6}$$

$$P_i = \frac{P}{\beta - 1}\left[y_p\beta\left(1 - \frac{1}{\beta^{N-i+1}}\right) + (1 - y_p)\left(\beta^{N-i+1} - 1\right)\right] \tag{7}$$

$$y_i = z_{i+1} = x_{i+2} = \frac{y_p}{y_p + \beta^{N-i}(1 - y_p)} \tag{8}$$

where i varies from *1* to N. L_i and V_i represent the tail and head flows in the depleted and enriched streams, respectively. For the stripping section, these equations are given by Cohen (1951)

$$W_i = \frac{W}{\beta - 1}\left[x_w\left(\beta^i - 1\right) + (1 - x_w)\beta\left(1 - \beta^{-i}\right)\right] \tag{9}$$

$$P_i = \frac{W}{\beta - 1}\left[x_w\beta\left(\beta^i - 1\right) + (1 - x_w)\left(1 - \beta^{-i}\right)\right] \tag{10}$$

$$x_i = z_{i-1} = y_{i-2} = \frac{\beta^{i-1}x_w}{1 + x_w\left(\beta^{i-1} - 1\right)} \tag{11}$$

where i varies from *1* to M. It can be shown that for all cases:

$$F_i = \frac{(1+\beta)P_i}{1 + z_i(\beta - 1)} = \frac{(1+\beta)W_i}{\beta - z_i(\beta - 1)} \tag{12}$$

The stage enrichment is defined as the ratio between the molar concentration of the component of interest leaving a stage and the corresponding concentration of the same component entering as feed into that stage. The stage recovery is defined as the number of moles of the species of interest withdrawn as product from a stage divided by the number of moles of that component fed to that stage. For the head flows, the stage enrichment (E_i) and recovery (R_i) are given by

$$E_i = \frac{y_i}{z_i} = \frac{\beta}{1 + z_i(\beta - 1)} \tag{13}$$

$$R_i = \frac{y_i P_i}{z_i F_i} = \frac{\beta}{1 + \beta} \tag{14}$$

For the tail flows, the stage depletion (D_i) and loss (L_i) are given by

$$D_i = \frac{x_i}{z_i} = \frac{1}{\beta - z_i(\beta - 1)} \tag{15}$$

$$L_i = \frac{x_i W_i}{z_i F_i} = \frac{1}{1 + \beta} \tag{16}$$

It is noteworthy that the recovery (R_i) and losses (L_i) are independent of the stage.

Step III involves determining the stage throughput θ_i and the overall throughput $\theta_{overall}$ of the process. Generally, the stage or overall throughput is defined as the amount of feed processed by the stage or cascade per unit time per unit mass of adsorbent utilized by the stage or

cascade. These throughputs are related to each other according to

$$\theta_{overall} = \frac{F}{\sum_{i=1}^{N_T} \frac{F_i}{\theta_i}} \tag{17}$$

Processes with higher throughputs imply less adsorbent inventory and smaller beds, thereby resulting in potential capital cost savings. Hence, the physical size of each PSA stage within an ideal cascade can be determined once the stage throughputs are determined.

For the 3-bed 3-step PSA cycle shown in Fig. 3, the stage throughput and the heavy and light product flows are defined as

$$\theta_i = \frac{F_i}{3v_i\rho_b} \tag{18}$$

$$HP_i = \frac{n_i(1 - R_{R,i})}{t_{step}} \tag{19}$$

$$LP_i = F_i - HP_i \tag{20}$$

where v_i is the volume of one of the beds, ρ_b is the bulk density of the adsorbent in the bed, $R_{R,i}$ is the reflux ratio defined earlier, and n_i is the total number of moles leaving a bed during the CnD step.

The stage throughput θ_i is determined from performance curves that are independently determined from a single PSA process. These performance curves consist of plots of the enrichment, recovery and/or separation energy against any parameter of interest. The parameter of interest could be the throughput, feed concentration, pressure ratio, cycle time or even the recycle ratio defined for the PSA cycle in Fig. 3. In this case throughput is chosen, wherein a stage throughput θ_i is sought that makes the enrichment and recovery match the values predicted by Eqs. 13 and 14 for a given feed concentration z_i. If the species of interest is the more strongly adsorbed one, then the stage P_i is HP_i in Eq. 19. If the species of interest is the more weakly adsorbed one, then the stage P_i is LP_i in Eq. 20.

It must be emphasized that these performance curves do not depend on the size of the PSA unit. Thus, the simulations are not necessarily carried out at the flow rates predicted by Eq. 12; both the volume of the bed and the feed flow rate can be arbitrarily selected for these simulations. Once the performance curves are established over a range of conditions and once the throughput is determined by matching the enrichment and the recovery to Eqs. 13 and 14 (as noted above), the bed volume v_i for stage i is calculated simply from Eq. 18.

These performance curves are determined in the customary way by using an in-house developed dynamic adsorption process simulator (DAPS). DAPS utilizes DASPK (van Keken et al. 1995) as a solver platform, which is built for solving complex partial differential equations via the method of lines and a time adaptive integration technique. The boundary conditions and main equations described by mass and energy balances, mass and energy transfer equations, and equilibrium isotherm relationships formulated in DAPS are reported elsewhere (Bhadra and Ebner 2013).

2.4 Dilute systems

The numerical approach just described for Step III can be simplified greatly for dilute systems. First, by neglecting $z_i(\beta - 1)$ in Eqs. 13 and 15 as z_i is very small, the enrichment and depletion and the recovery and loss all become constants throughout the cascade, i.e.,

$$E_i = \beta \tag{21}$$

$$D_i = \frac{1}{\beta} \tag{22}$$

Furthermore, the performance curves of the PSA process become independent of the feed concentration. Because of this fact and the fact that both E_i and R_i are only functions of β (see Eqs. 14 and 21), all the stages in the cascade operate at the same stage throughput $\theta_i = \theta$ and the same stage recycle ratio $R_{Ri} = R_R$. This allows the overall throughput $\theta_{overall}$ and stage single bed volume v_i in Eq. 18 to be calculated from Eqs. 23 and 24, respectively.

$$\theta_{overall} = \frac{F}{\sum_{i=1}^{N_T} F_i}\theta \tag{23}$$

$$v_i = \frac{F_i}{3\theta\rho_b} \tag{24}$$

3 Results and discussion

The methodology described above is illustrated with the design of an ideal cascade of PSA units for the isotopic separation of a gas stream containing only pure CO. The problem involves the enrichment and removal of ^{14}CO, the more strongly adsorbed species, from its own isotopic mixture of all three isotopes. The species of interest is thus ^{14}CO in the ideal cascade. It must be noted that because binary ideal cascade theory is utilized in this work, it is assumed that the presence and slight enrichment of ^{13}CO does not influence the performance of the ^{14}CO throughout the cascade. The justification for this assumption is given below. Similarly, this study does not consider the effect of the isotopic distribution of oxygen in CO, namely ^{16}O, ^{17}O and ^{18}O. Because ^{17}O and ^{18}O are present in very low fractions (<1 %), any CO species containing these oxygen

isotopes necessarily operates in the Henry's law region which obviates its influence on the behavior of ^{14}CO.

A primary feed flow rate of 100 mol/h (i.e., 2240 L_{STP}/h) containing 1 ppm (i.e., $z_F = 1.0 \times 10^{-6}$) of ^{14}CO is processed to produce a heavy product stream enriched 20 times in this isotope (i.e., $y_p = 2.0 \times 10^{-5}$). The feed concentrations of the other two isotopic species are given in Table 1. Table 1 also lists the adsorbent and PSA bed properties, as well as the thermodynamic properties based on the Toth equilibrium adsorption isotherm and the kinetic properties based on a linear driving force (LDF) model for this adsorbate (CO)—adsorbent (NaX) system (Izumi et al. 2005; Bhadra and Ebner 2013). Notice that the relative affinity of ^{13}CO for NaX is significantly closer to ^{12}CO than it is to ^{14}CO. This indicates that ^{13}CO does not enrich much throughout the cascade and because its feed concentration is so low it also indicates that its equilibrium adsorption isotherm remains in the Henry's law region, thereby eliminating any effect on the performance of ^{14}CO throughout the cascade. Overall, these assertions make the three isotopes behave like two isotopes, which allow binary ideal cascade theory to be applicable to such a system.

As indicated earlier, all the PSA units (stages) in the ideal cascade are based on the 3-bed 3-step cycle schedule shown in Fig. 3. Following the basic operating conditions of Izumi et al. (2005) each PSA unit operates with external and feed temperatures of 227.59 K, a high pressure of 120 kPa, and a low pressure of 1 kPa. The total cycle time for each PSA unit is chosen to be 7200 s, which makes the duration of each step equal to 2400 s. The ideal cascade

Table 1 Bed, adsorbent, adsorbate and process characteristics and properties

Bed characteristics	
Bed radius[a] (m)	0.025
Bed length[a] (m)	0.75
Bed porosity	0.32
Bulk density (kg/m^3)	690.0
Heat transfer coefficient (kW/m^2/K)	0.0067
Adsorbent characteristics	
Adsorbent	NaX Zeolite
Pellet radius (m)	0.0008
Pellet density (kg/m^3)	1357.0
Pellet void fraction	0.39
Solid heat capacity (J/kg/K)	920.0
Process characteristics	
Primary feed flow (L(STP)/h)	2240
Primary feed mole fraction: ^{12}CO, ^{13}CO and ^{14}CO	0.980009, 0.01999, 0.000001
Feed temperature (K)	227.59
Wall temperature (K)	227.59
High pressure (kPa)	120.0
Low pressure (kPa)	1.0
Equilibrium[b] and kinetic[c] information	
B_i for ^{14}CO, ^{13}CO and ^{12}CO (K)	85.5, 85.5, 85.5
b_{i0} for ^{14}CO, ^{13}CO and ^{12}CO (kPa^{-1})	0.0305, 0.0280, 0.0273
q_i^{st} for ^{14}CO, ^{13}CO and ^{12}CO (mol/kg/K)	−0.03, −0.03, −0.03
q_i^{s0} for ^{14}CO, ^{13}CO and ^{12}CO (mol/kg)	9.91, 9.91, 9.91
n_i^t for ^{14}CO, ^{13}CO and ^{12}CO (K)	260.9, 260.9, 260.9
n_i^0 for ^{14}CO, ^{13}CO and ^{12}CO	−0.43, −0.43, −0.43
Heat of adsorption for all CO isotopes (kJ/mol)	13.95
k_{LDFi} for ^{14}CO, ^{13}CO and ^{12}CO (s^{-1})	1.0, 1.0, 1.0

[a] Values used in the dynamic adsorption process simulator (DAPS)

[b] The isotherm is defined according to the Toth mixed gas isotherm: $q_i^* = \frac{b_i P_i q_i^s}{\left(1+\left(\sum_j^3 b_j P_j\right)^{n_i}\right)^{\frac{1}{n_i}}}$ with $b_i = b_{io}\exp\left(\frac{B_i}{T}\right)$; $q_i^s = q_i^{s0} + q_i^{st}T$; $n_i = n_i^0 + \frac{n_i^t}{T}$

[c] The kinetic model is based on the linear driving force formulation: $\frac{\partial \bar{q}_i}{\partial t} = k_{LDF,i}\left(q_i^* - \bar{q}_i\right)$

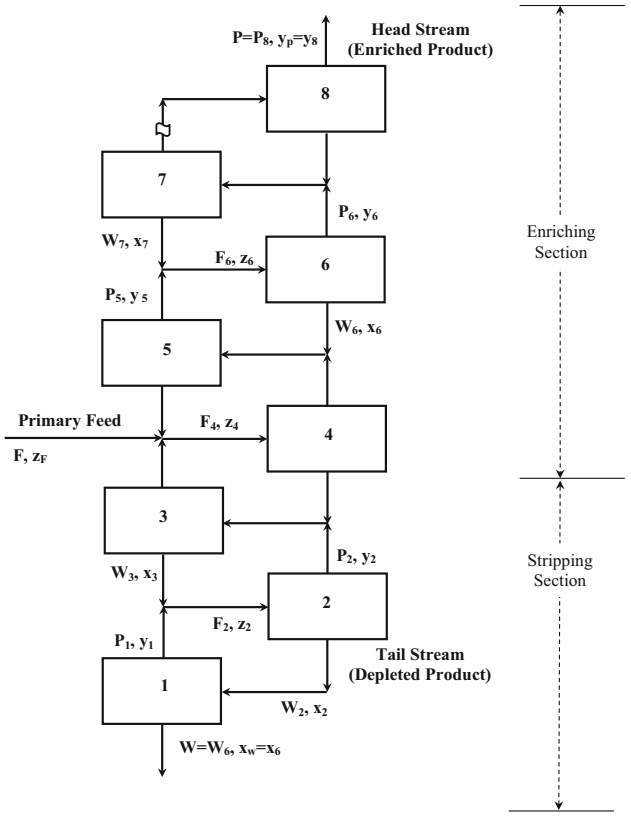

Fig. 4 Schematic representation of an ideal cascade for a configuration with $M = 3$ and $N = 5$, where M and N correspond to the total number of stages in the stripping and enriching sections, respectively. The primary feed is supplied to stage 4

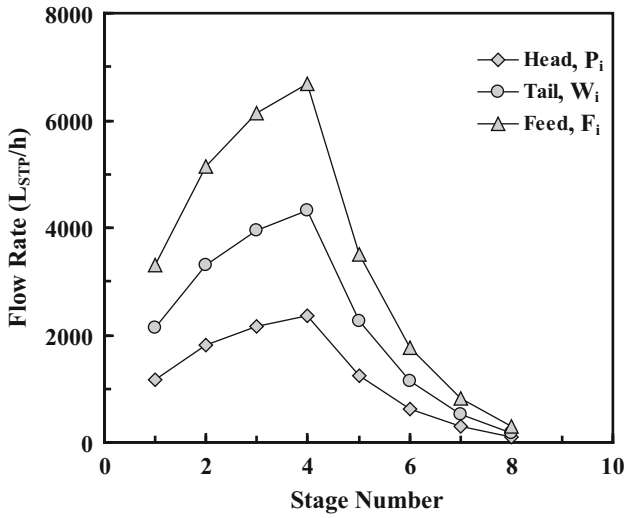

Fig. 5 Flow rate of head, tail and feed streams as a function of stage number, based on the ideal cascade configuration shown in Fig. 4

consists of 3 PSA units in the stripping section ($M = 3$) and 5 PSA units in the enriching section ($N = 5$), with these numbers chosen arbitrarily to demonstrate the procedure. This 8 stage, ideal cascade is shown in Fig. 4.

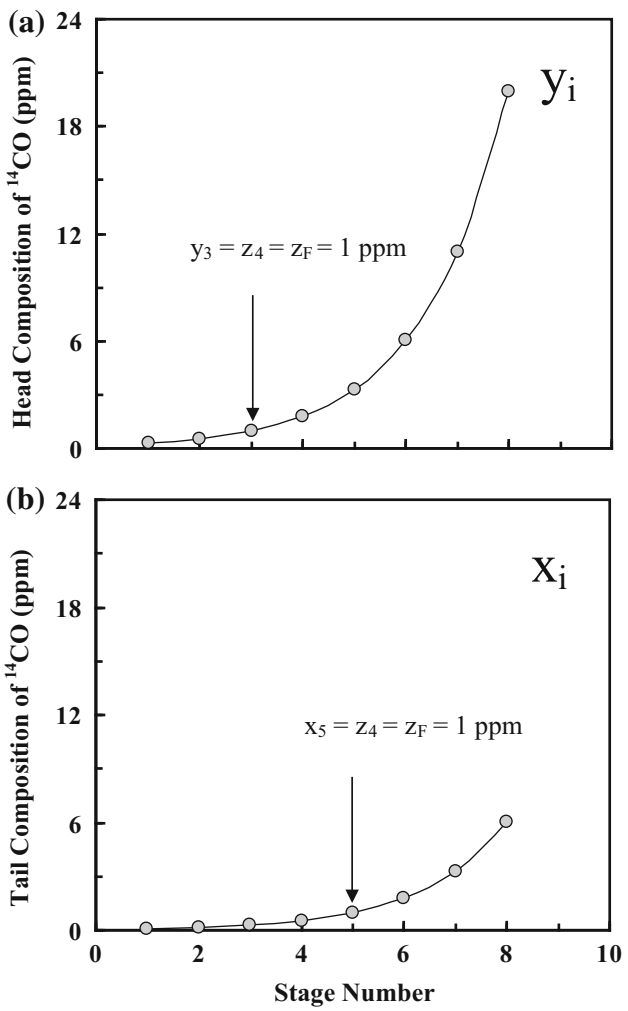

Fig. 6 Concentration of ^{14}CO in the **a** head (enriched) and **b** tail (depleted) streams as a function of stage number, based on the ideal cascade configuration shown in Fig. 4

Step I is initialized by solving Eqs. 4 and 5. With the defined values of M, N, z_F and y_p, the head (or tail) separation factor β and the tail product ^{14}CO mole fraction x_w are computed and equal to 1.82 and 9.1×10^{-8} (i.e., 0.091 ppm), respectively. With the primary feed flow being 2240 L_{STP}/h, the overall and ^{14}CO mass balances over the cascade result in head P and tail W flow rates of 102.37 and 2137.63 L_{STP}/h, respectively. These overall flow rates and compositions restrict the overall ^{14}CO recovery R in the enriched product P to be 91.4 %.

Step II is initialized by solving Eqs. 6–11. The corresponding results for the stage flow rates and compositions of the more strongly adsorbed component ^{14}CO as a function of the cascade stage number are shown in Figs. 5 and 6, respectively. Stages 1–3 represent the stripping section of the cascade and stages 4–8 represent the enriching section of the cascade. The primary feed enters the cascade at stage 4 (i.e., $M + 1$).

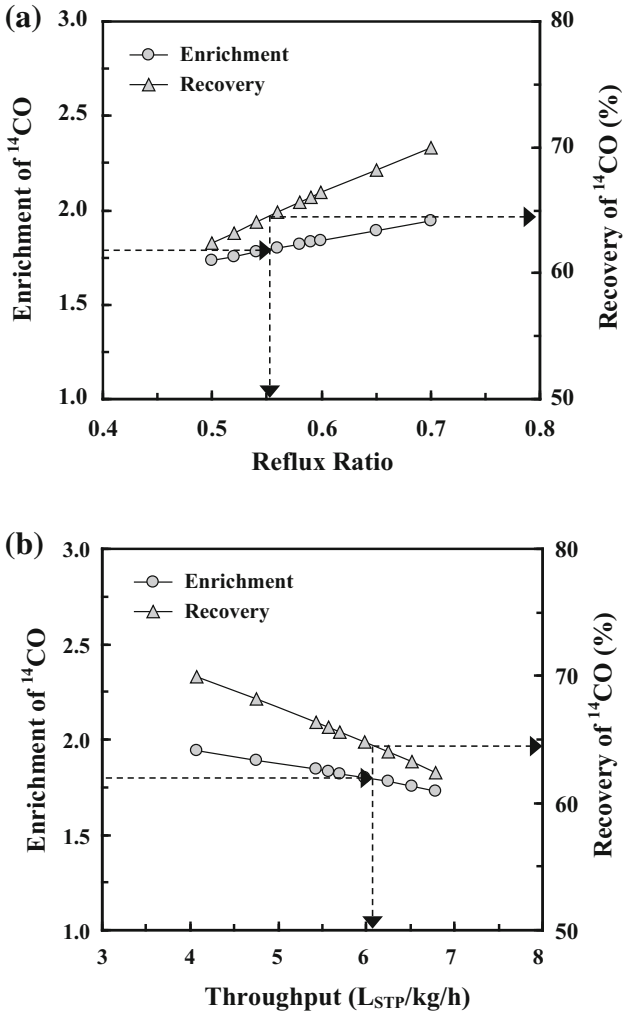

Fig. 7 Stage enrichment and recovery of ^{14}CO as a function of the **a** reflux ratio and **b** throughput θ for a PSA unit receiving feed with a composition identical to that of the primary feed fed to the cascade of PSA units. The PSA unit is based on the 3-bed 3-step PSA process shown in Fig. 3

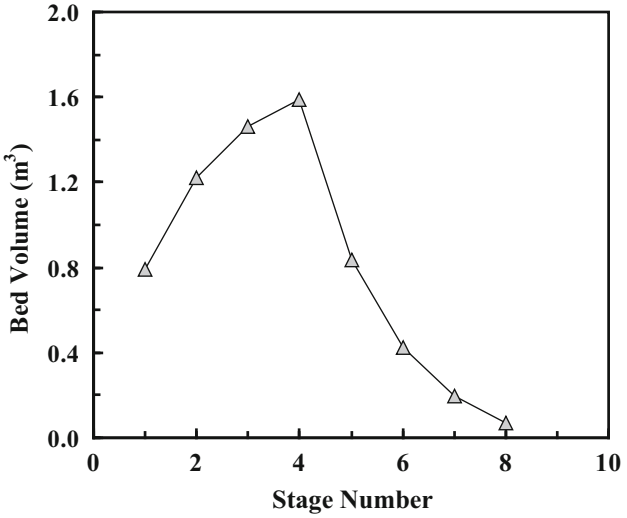

Fig. 8 Single PSA bed volume required in each stage (PSA unit) of the cascade of PSA units to enrich ^{14}CO to the target value of 20 ppm, based on the ideal cascade configuration shown in Fig. 4

Figure 5 shows that stage 4 is where a maximum occurs for all inter-stage flow rates, whether associated with the head, tail or feed. In addition, the tapered shape of the ideal cascade is quite apparent, as the inter-stage flow rate rapidly diminishes as the head and tail end stages are approached. Figure 6 shows how the ^{14}CO concentration in both the head and tail streams increases with stage number and that the composition of ^{14}CO in the head stream of stage 8 is exactly 20 ppm as specified (i.e., $y_p = 2.0 \times 10^{-5}$). It can easily be verified from this figure that the non-mixing criterion (i.e., $z_i = y_{i-1} = x_{i+1}$) is being satisfied throughout the cascade, even for the stage where the streams collectively mix with the primary feed (i.e., $z_4 = y_3 = x_5 = z_F = 1.0 \times 10^{-6}$).

Figure 7 shows the performance curves obtained for the PSA process defined in Fig. 3. These performance curves are expressed in terms of the ^{14}CO enrichment E and ^{14}CO recovery R in the head product P as a function of the reflux ratio R_R and the throughput θ for the single PSA unit described in Table 1. These results are obtained by varying the reflux ratio R_R between 0.5 and 0.7 while R and E are obtained as outputs from DAPS at the periodic state and θ is calculated from Eq. 18. As indicated earlier, the results from these simulations are obtained using an arbitrary bed volume and flow rate. The bed volume is based on that given in Table 1 and the feed flow rate is estimated from the moles n leaving the CnD step according to the same heuristic expression developed elsewhere (Bhadra and Ebner 2013) and given by Eq. 25.

$$F = 20\frac{n(1-R_R)}{t_{step}} \tag{25}$$

The results in Fig. 7 are also assumed to be valid for any feed concentration throughout the cascade, because the system is dilute and not affected by the degree of enrichment of ^{13}CO, as discussed above. In this case, the ^{14}CO concentration in the feed is 1 ppm.

Only one solution is required for the entire cascade, namely one unique set of E, R, R_R and θ from the curves in Fig. 7. While the determination of this set of parameters is explained below, it is noteworthy that it is the same for each stage, i.e., each PSA unit in the cascade, because of the dilute concentration of ^{14}CO. Hence, the results in Fig. 7, as well as the relationships in Eq. 14, and then Eqs. 21, 23 and 24 for dilute systems, are valid for use in Step III, as follows.

Step III is initialized by using the results in Fig. 7b to determine the stage throughput θ for which the enrichment

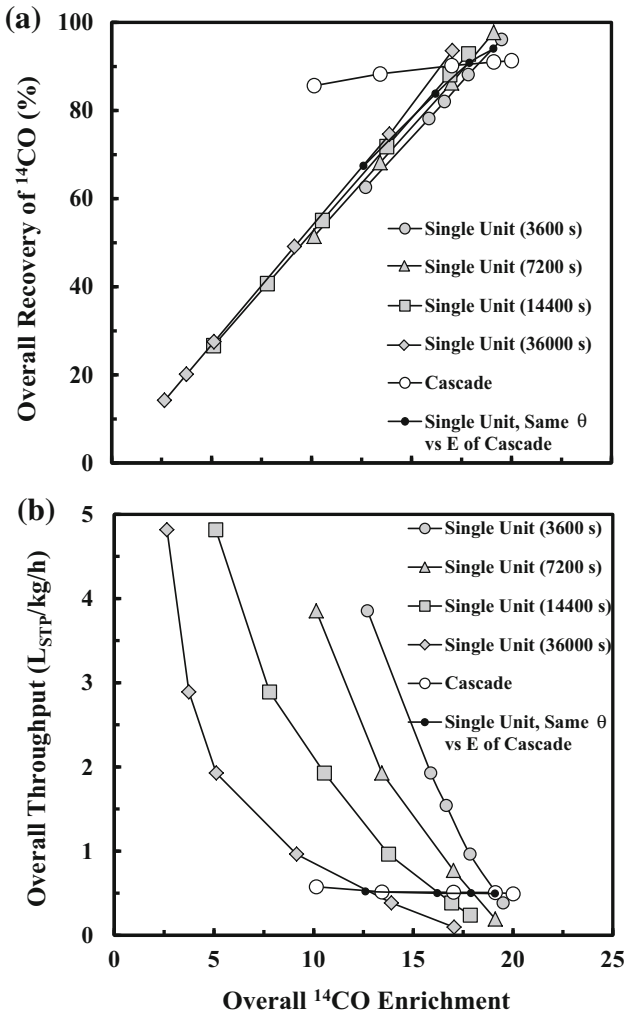

Fig. 9 Comparison of a single PSA unit to a cascade of PSA units: **a** overall recovery of ^{14}CO and **b** overall throughput, both as a function of overall ^{14}CO enrichment. Each PSA unit, whether alone or in a cascade, consists of the 3-bed 3-step PSA process shown in Fig. 3. The results for the single PSA unit where obtained at four different cycle times and one where both the overall throughput and overall enrichment match those of the cascade of PSA units. The cycle time for all the PSA units in the cascade is 2400 s. The results for the ideal cascade are based on the configuration shown in Fig. 4

E is equal to the separation factor β, as indicated by Eq. 21. Thus, in this example, for $E = \beta = 1.82$, Fig. 7 provides $\theta = 6.09$ L_{STP}/kg/h and a corresponding $R_R = 0.556$. It is noteworthy that the results in the figure are consistent with $R = \beta/(1 + \beta) = 64.5$ %, as expected from mass conservation. The arrows in the figure indentify these unique values. Now, with the interstage feed flow rates given in Fig. 5 and the just obtained stage thoughput θ, Eqs. 23 and 24 are used to obtain $\theta_{overall} = 0.49$ L_{STP}/kg/h and the stage (single) bed volumes shown in Fig. 8. It is not surprising that the size of a single PSA bed is at a maximum where the primary feed is introduced, again revealing the tapered characteristic of the ideal cascade.

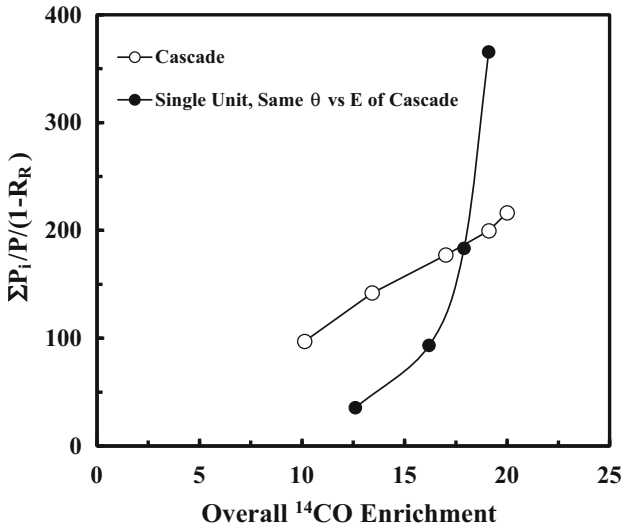

Fig. 10 Comparison of a single PSA unit to a cascade of PSA units in terms of the ratio between total recompressed flows to product flow (proportional to power consumption) as a function of the overall ^{14}CO enrichment. The values for the single PSA unit are obtained from the results depicted by the black circles shown in Fig. 9. For a single PSA unit $\Sigma P_i/P = 1$. The results for the ideal cascade are based on the configuration shown in Fig. 4

Now that the 3-step methodology for applying cascade theory to a PSA process is established, it is desirable to compare the performance of an ideal cascade of PSA units to a single PSA unit. This is accomplished by simulating a single PSA unit that encompasses the performance range of an ideal cascade of PSA units. Then, these results are interpolated to find the single PSA unit that exactly matches the performance of the ideal cascade of PSA units in terms of overall throughput and overall enrichment, as follows.

First, the performance of an ideal cascade of PSA units is obtained for overall enrichments E of 10.1, 13.4, 17.0, 19.1 and 20.0 utilizing the same cascade of Fig. 4, the same PSA configuration shown in Fig. 3, and the same feed conditions and parameters listed in Table 1. The corresponding R_R for these increasing values of enrichments are 0.335, 0.465, 0.508, 0.532 and 0.556. Recall that the case where $E = 20$ and $R_R = 0.556$ corresponds to the cascade just analyzed. To achieve the same overall ^{14}CO recoveries, throughputs and ^{14}CO enrichments in the single PSA units as obtained in the ideal cascades of PSA units, the performances of several single PSA units are obtained at cycle times of 3600, 7200, 14200 and 36000 s. The same procedure utilized to obtain the results in Fig. 7 is exploited here but over a wider range of R_R. For increasing values of overall enrichments, the R_R are arbitrarily chosen to be 0.98, 0.99, 0.992, 0.995 and 0.998 for the 3600 s cycle time unit; 0.96, 0.98, 0.992 and 0.998 for the 7200 s cycle time unit; 0.9, 0.94, 0.96, 0.98, 0.992 and 0.995 for

the 14200 s cycle time unit; and 0.75, 0.85, 0.9, 0.95, 0.98 and 0.995 for the 36000 s cycle time unit. The results obtained for the ideal cascades of PSA units, along with those obtained for the single PSA units, are shown in Fig. 9.

The single PSA unit that provides the same overall throughput $\theta_{overall}$ and same overall enrichment as the ideal cascade of PSA units is obtained by finding the overall recovery for a single PSA unit from one of the overall recovery versus overall enrichment curves in Fig. 9a for which the corresponding single PSA unit overall throughput versus overall enrichment curve intersects the curve for the ideal cascade of PSA units in Fig. 9b. These new curves for the single PSA unit that now match the performance of the ideal cascade of PSA units in terms of overall throughout and overall enrichment are identified by solid black circles in Fig. 9a and b. These new curves represent a single PSA unit where both the cycle time and reflux ratio are adjusted so that its overall throughput versus overall enrichment curve exactly coincides with that of the ideal cascade of PSA units as shown in Fig. 9b.

It is interesting that the new overall recovery versus overall enrichment curve for the single PSA unit in Fig. 9a differs significantly from than that of the ideal cascade of PSA units. Below an overall enrichment of about 18, where the two curves intersect, the curve for the single PSA unit displays a markedly steeper slope with increasingly lower overall recoveries as the overall enrichment decreases below 18. At overall enrichments higher than 18 the single PSA unit exhibited only slightly higher overall recoveries than the cascade of PSA units. These results are significant as they show the potential of an ideal cascade of PSA units to perform better than a single PSA unit over a wide range of overall enrichments. However, this apparent advantage of an ideal cascade of PSA units comes at a cost.

Figure 10 displays the ratio of the sum of the enriched product flows that leave the CnD step of each stage, i.e., $\Sigma P_i/(1 - R_R)$ to the head product for the cascade or the single PSA units, i.e., P. Note that for the single PSA units the $\Sigma P_i/P$ is equal to unity. Also note that the enriched product flows must necessarily be compressed to the feed pressure before they are sent back to the HR step in a PSA unit, or sent as part of the FP/F step of the next stage in case of the cascade, or sent as head product P in the case of the last stage $N + M$ in the cascade. Thus, the resulting variable $\Sigma P_i/(P(1 - R_R))$ reflects how much power is spent in producing P and is thus a direct measure of the operating cost of the system. Notice that all the values of this flow ratio are quite large. This is indicative of the intrinsic low adsorption selectivity for this separation that requires exceedingly large reflux ratios to achieve any enrichment.

The results in Fig. 10 show that at the conditions where the cascade of PSA units outperforms the single PSA unit (i.e., at overall enrichments below about 18, as shown in Fig. 9a), the cascade is more costly to operate. In contrast, at the higher overall enrichments, where the single PSA unit performs only slightly better than the cascade (as shown in Fig. 9a), the single PSA unit now becomes more costly to operate. These results, not surprisingly, show that the better performing system always incurs higher operating costs. More importantly, these results tend to show that a cascade of PSA units may be more advantageous than a single PSA unit, depending on the desired performance, as long as the capital and operating costs are acceptable.

4 Conclusions

The ideal cascade approach represents a separation process design that minimizes inter-stage flow and thus cost for a specific application. When the separation is done by PSA, each stage within an ideal cascade consists of a series of different sized, multi-bed PSA units. In this work, a three-step design methodology was developed for applying binary ideal cascade theory to PSA via simulation.

The three steps involved: (I) establishing the number of stages, the stage separation factor and overall performance variables of the cascade; (II) determining all internal flows as well as compositions and stage performance variables, such as recoveries, losses, enrichments and depletions in the cascade; and (III) determining stage and overall throughputs of the cascade. This three-step methodology was applied to the enrichment of ^{14}CO from 1 to 20 ppm in a mixture of its own three isotopes. Binary ideal cascade theory was considered to be valid because ^{12}CO and ^{13}CO exhibited very similar affinities for NaX, which limited its enrichment to be within the Henry's law region of its isotherm thereby eliminating any effect on the performance of ^{14}CO throughout the cascade. The dilute solution approximation was also valid for this system, which simplified the design by making the performance of each stage in the cascade the same, i.e., each stage had the same throughput, ^{14}CO recovery and ^{14}CO enrichment.

An 8 stage cascade was analyzed, with 3 stages in the stripping section, 5 stages in the enriching section and the feed fed to stage 4. Each stage consisted of a 3-bed 3-step PSA process of varying size, all utilizing FP/F, HR and CnD steps of equal duration, and the same total cycle time. The stage and overall throughputs were obtained via simulation of this 3-bed 3-step PSA process with the aid of DAPS (a dynamic adsorption process simulator developed in-house). The performance in terms of overall ^{14}CO recovery from an ideal cascade of PSA units was compared to that from a single PSA unit operating with the same overall ^{14}CO enrichment and same overall throughput as the cascade.

The results showed that the cascade of PSA units compared to the single PSA unit exhibited increasingly higher overall recoveries as the overall enrichment decreased; the performance of both systems became identical at an overall enrichment of about 18; and at overall enrichments higher than 18 the single PSA unit exhibited only slightly higher overall recoveries than the cascade of PSA units. In either case the better performing separation process always required more power to operate. In general, This analysis showed how to design an ideal cascade of PSA units for binary isotope separation and that a cascade of PSA units may be more advantageous than a single PSA unit, depending on the desired performance and as long as the capital and operating costs are acceptable.

Acknowledgments The authors gratefully acknowledge financial support provided in part by the National Space Biomedical Research Institute through NASA NCC9-58, in part by the SAGE Center at the University of South Carolina, and in part by the Process Science and Technology Center, a consortium composed of the University of Texas at Austin, the University of South Carolina, and the Texas A&M University.

References

Ambartsumian, R.V., Letokhov, V.S., Ryabov, E.A., Chekalin, N.V.: (1975) Isotopic selective chemical reaction of BCl3 molecules in a strong infrared laser field. ZhETF Pisma Redaktsiiu. **20**, 597 (1974)

Applegate, L.E.: Membrane separation processes. Chem. Eng. **91**, 64 (1984)

Benedict, M., Pigford, T.H., Levi, H.W.: Nuclear Chemical Engineering, 2nd edn. McGraw-Hill, NY (1981)

Bhadra, S.J., Ebner, A.D., Ritter, J.A.: Carbon monoxide isotope enrichment and separation by pressure swing adsorption. Adsorption **19**, 11 (2013)

Chang, F.H., Vogt, H.K., Krochmalnek, L.S., Sood, S.K., Bartoszek, F.E., Woodall, K.B., Robins J.R.: Producing carbon-14 isotope from spent resin waste. US Patent 5,286,468, 1994

Cheh, C.H.: Advances in preparative gas chromatography for hydrogen isotope separation. J. Chromatogr. A **658**, 283 (1994)

Cohen, K.: The theory of isotope separation separation as applied to the large scale production of uranium. McGraw-Hill, New York (1951)

Cohen, K., Kaplan, I.: Absolute efficiencies of isotope separation by counter-current centrifuges: a new counter-current centrifuge. Report No. A-101, Columbia University, New York, 1942

Fachinger, J., Lensa, W.V., Podruhzina, T.: Decontamination of nuclear graphite. Nucl. Eng. Des. **238**, 3086 (2008)

Geankoplis, C.J.: Transport Processes and Separation Process Principles, 4th edn. Prentice-Hall, Upper saddle River (2003)

Hill, F.B., Grzetic, V.: Cascades for hydrogen isotope separation using metal hydride. J. Less-Common Met. **89**, 399 (1983)

Horen, A.S., Lee, M.W.: Metal hydride based isotope separation—Large scale operations. In: Proceedings of the Fourth ANS Topical Meeting on Tritium Technology in Fission, Fusion and Isotopic Applications, New Mexico, 1991

Izumi, J., Yasutake, A., Kobayashi, S., Shikichi, A., Kinugasa, A., Kohanawa, O., Okumura, N., Kanda, T., Izumi, Y., Saigusa, M., Oguri, D., Inoue, T., Oumori, S.: ^{14}CO and ^{12}CO separation on Na-X using pressure swing adsorption at low temperatures. Adsorption **11**, 817 (2005)

Keshaviah, V.R., C.E. Jr. Hamrin: Progress Report, U.S. Atomic Energy Commission. Rept. No. ORD-3913-2, 1972

Kholpanov, L.P., Sulaberidze, G.A., Potapov, D.V., Chuzhinov, V.A.: Multicomponent isotope separating cascade with losses. Chem. Eng. Proc. **36**, 189 (1997)

Letokhov, V.S.: USSR Patent N 65743, 1970

Lonsdale, H.K.: The growth of membrane technology. J. Membr. Sci. **10**, 81 (1982)

Mason, J.B., Bradbury, D.: Process for the treatment of radioactive graphite. US Patent 6,625,248, 2002

McInteer, B.B.: Fractional Distillation for Carbon Isotope. Separation. Las Alamos National Laboratory Report, LANL-78-76, 1978

O'Farrell, P.H.: Method of isotope enrichment. US Patent 4,290,855, 1981

Ortman, M.S., Heung, L.K., Nobile A., Rabun, R.L.: Tritium processing at the Savanah River Site (SRS): Present and future. In: Proceedings of the 36th National Symposium of the American Vacuum Society, MA, 1989

Patrick, R.R., Schrodt, J.T., Kermode, R.I.: Thermal parametric pumping of air-SO_2. Separation Sci. **7**, 331 (1972)

Pratt, H.R.C.: Countercurrent separation processes. Elsevier, Amsterdam (1967)

Robieux, J., Auclair, J.M.: Separation of isotopes. French Patent 1,391,738, 1965

Shanahan, K.L., Holder, J.S., Wermer, J.R.: Tritium aging effects in palladium on kieselguhr. J. Alloy. Compd. **293–295**, 62 (1999)

van Keken, P.E., Yuen, D.A., Petzold, L.R.: DASPK: A new high order and adaptive time-integration technique with applications to mantle convection with strongly temperature-and pressure-dependent rheology. Geophys. Astrophys. Fluid Dyn. **80**, 57 (1995)

Whitley, S.: Review of the gas centrifuge until 1962. Part I: Principles of separation physics. Rev. Modern Phys. **1984**(56), 41 (1984)